Generation of pressures over 40 GPa using Kawai-type multi-anvil press with tungsten carbide anvils

' , , , , D. Druzhbin, R. Myhill, , , , , , , , , and

Citation: Rev. Sci. Instrum. **87**, 024501 (2016); doi: 10.1063/1.4941716
View online: http://dx.doi.org/10.1063/1.4941716
View Table of Contents: http://aip.scitation.org/toc/rsi/87/2
Published by the American Institute of Physics

Generation of pressures over 40 GPa using Kawai-type multi-anvil press with tungsten carbide anvils

T. Ishii (石井 貴之),[1,2,a)] L. Shi (史 兰兰),[1] R. Huang (黄 琼),[1] N. Tsujino (辻野 典秀),[3] D. Druzhbin,[1] R. Myhill,[1] Y. Li (李 杨),[1] L. Wang (王 林),[1] T. Yamamoto (山本 貴史),[4] N. Miyajima (宮島 延吉),[1] T. Kawazoe (川添 貴章),[1] N. Nishiyama (西山 宣正),[5] Y. Higo (肥後 祐司),[6] Y. Tange (丹下 慶範),[6] and T. Katsura (桂 智男)[1]

[1]*Bayerisches Geoinstitut, University of Bayreuth, 95440 Bayreuth, Germany*
[2]*Geodynamics Research Center, Ehime University, Matsuyama, Ehime 790-8577, Japan*
[3]*Institute for Study of the Earth's Interior, Okayama University, Misasa 682-0193, Japan*
[4]*Department of Earth and Planetary Systems Sciences, Graduate School of Science, Hiroshima University, Kagamiyama 1-3-1, Higashi-Hiroshima 739-8526, Japan*
[5]*Deutsche Electronen-Synchrotron (DESY), Notkestraße 85, 22607 Hamburg, Germany*
[6]*Japan Synchrotron Radiation Research Institute (JASRI), 1-1-1, Kouto, Sayo-cho, Sayo-gun, Hyogo 679-5198, Japan*

(Received 25 September 2015; accepted 25 January 2016; published online 16 February 2016)

We have generated over 40 GPa pressures, namely, 43 and 44 GPa, at ambient temperature and 2000 K, respectively, using Kawai-type multi-anvil presses (KMAP) with tungsten carbide anvils for the first time. These high-pressure generations were achieved by combining the following pressure-generation techniques: (1) precisely aligned guide block systems, (2) high hardness of tungsten carbide, (3) tapering of second-stage anvil faces, (4) materials with high bulk modulus in a high-pressure cell, and (5) high heating efficiency. © *2016 AIP Publishing LLC.* [http://dx.doi.org/10.1063/1.4941716]

I. INTRODUCTION

The Kawai-type multi-anvil press (KMAP) is a widely used high-pressure apparatus.[1] In this kind of apparatus, a sample is loaded in an octahedral pressure medium and compressed with eight inner (second-stage) anvils with corner truncations, which are compressed with six outer (first-stage) anvils synchronously. A sample is heated by a resistive furnace that is usually placed in a thermal insulator in a pressure medium. Heating elements are typically graphite, $LaCrO_3$, TiB_2, or noble metals with high melting points such as Re. Materials for the inner anvil and pressure medium are usually tungsten carbide (WC) and chromium-doped magnesia (MgO), respectively. Experiments conducted with this kind of apparatus tend to produce more reliable data than diamond anvil cell studies because of larger sample volumes and relatively stable and uniform heating. For these reasons, the KMAPs have been a popular tool for high-pressure solid geoscience and high-pressure synthesis of novel materials.

Pressures that can be routinely generated using KMAP are, however, usually limited to 25-28 GPa, corresponding to the top of the Earth's lower mantle.[2,3] This limitation is primarily a consequence of hardness of WC anvils. While for many years, the upper half of the lower mantle was considered relatively uninteresting; recent seismological studies[4] have shown that several subducted slabs penetrate into the lower mantle and stagnate at ~1000 km, corresponding to 40 GPa. It is therefore desired that chemical and physical properties of mantle minerals are investigated reliably at pressures over 40 GPa by using KMAP. Recent technological development of KMAP makes it possible to routinely generate pressures up to 60 GPa[5–7] by use of sintered diamond (SD) second-stage anvils. Even pressures over 100 GPa were achieved by the most advanced technique with SD anvils.[8] SD anvils are, however, extremely expensive, and therefore research groups that can purchase SD anvils and practically conduct experiments with them are limited. For this reason, we have developed techniques to simultaneously generate high temperatures and pressures exceeding 40 GPa using a KMAP with WC anvils.

Since we have succeeded in generating over 40 GPa pressures using tungsten carbide anvils for the first time in the world, we report the experimental techniques adopted in these high-pressure generations.

II. HIGH-PRESSURE APPARATUS

The KMAPs used in this study are SPEED-*Mk.*II at the synchrotron radiation facility, SPring-8 (BL04B1), Japan, and IRIS-15 at Bayerisches Geoinstitut, University of Bayreuth, Germany. Details of SPEED-*Mk.*II were already described elsewhere.[9] Therefore, those of IRIS-15 (Fig. 1) are described in this paper.

The concept of IRIS-15 is the same as that of SPEED-*Mk.*II. The high-pressure vessel was designed on the basis of the DIA-type guide block system[10,11] (Fig. 1(b)). The DIA-type guide block system consists of the upper and lower guide blocks with four 45° slopes and the four sliding wedges, each of which is equipped with an outer anvil. By uniaxial compression, the four wedges slide on the 45° slopes

a)Author to whom correspondence should be addressed. Electronic mail: takayuki.ishii@uni-bayreuth.de. This research was performed while T. Ishii was at Bayerisches Geoinstitut, University of Bayreuth, 95440 Bayreuth, Germany.

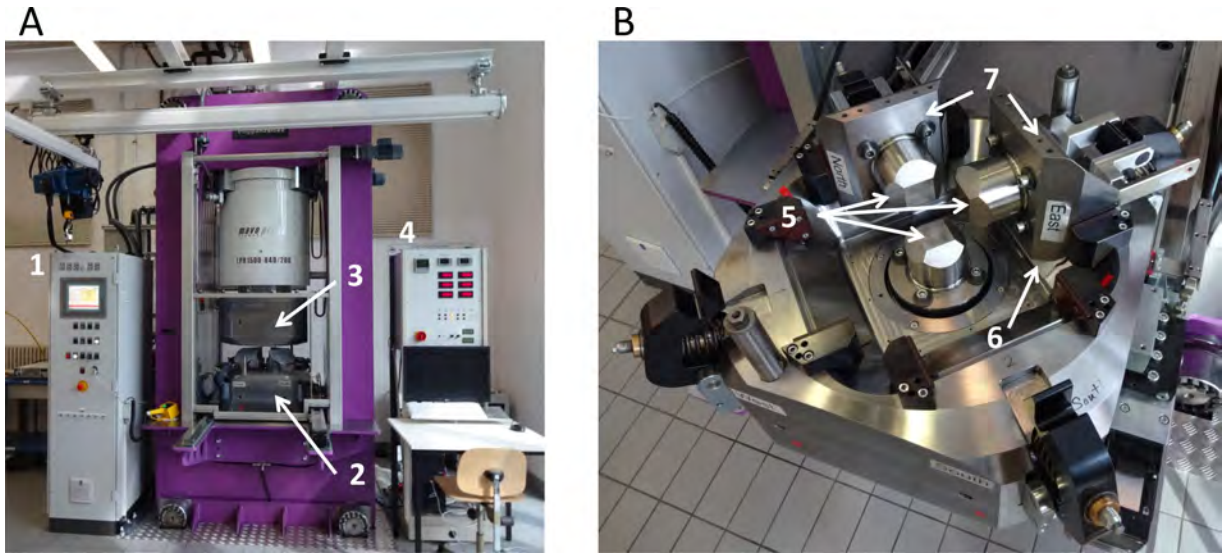

FIG. 1. Photographs of IRIS-15. (a) Overview and (b) the lower guide block with two sliding wedges. (1) Load control system, (2) lower guide block, (3) upper guide block, (4) heating system, (5) outer (first-stage) anvils, (6) Teflon sheet, and (7) the sliding wedges placed on the 45° slope. In (b), the other two sliding wedges are not placed to show the bottom outer anvil.

of the guide blocks, and the six outer anvils synchronously compress the central cubic space. A Kawai-type assembly consisting of eight inner WC anvils with truncated corners and an octahedral pressure medium with a sample is placed in the cubic space. Currently, the outer anvils are made of hardened steel with a truncated edge length of 50 mm. The inner WC anvils have an edge length of 26 mm.

As is discussed in the work Katsura *et al.*,[9] the main problem with the DIA-type guide block system for high-pressure generation by the above compression style is that press loads distort the geometry of the space compressed by the outer anvils. In general, this compression space has a tetragonal symmetry rather than cubic, because the strengths for supporting the outer anvils are different between the guide blocks and the sliding wedges. This circumstance changes difference in vertical and horizontal dimensions with increasing press load, which results in stress asymmetry within the compression space to greatly increase probability of blow-out. In order to suppress this problem, a cavity was made in each guide block to control the strength supporting the top and bottom outer anvils (Fig. 2). The size of the cavity was adjusted by repeatedly compressing stainless blocks so that the horizontal and vertical dimensions of the compression space formed by the outer anvils should ideally remain identical at any press load. Figure 3 shows the results of the adjustment of the compressional space. Through a series of adjustments, the changing rate in difference of the vertical dimensions from the horizontal ones with pressure has been reduced from 22 μm/MN to −0.07 μm/MN. This rate is smaller than those of SPEED-*Mk.*II (4 μm/MN) in the stage of Katsura *et al.*[9] and also MADONNA-II (2 μm/MN[12]), whose guide block is now installed in the frame of SPEED-*Mk.*II.

III. INNER ANVILS

A. Selection of carbide material

The hardness of anvil material is the most essential factor for high-pressure generation in KMAPs. The usual anvil

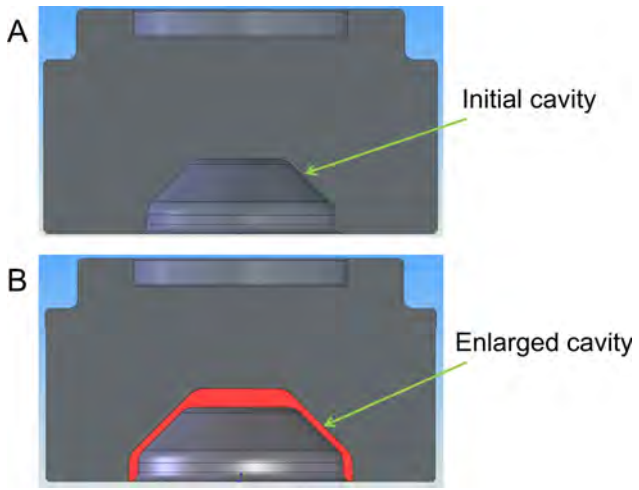

FIG. 2. Cross sections of the lower guide block (a) before and (b) after the 1st compression test. The red part in (b) denotes the increase of volume of the cavity in the guide block to suppress a relative increase of the vertical dimension to the horizontal one in the cubic compression space.

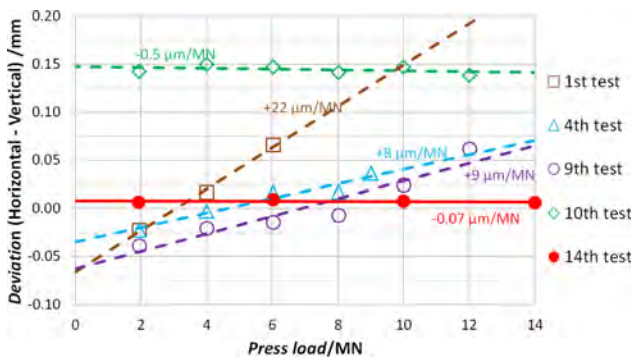

FIG. 3. Deviation of the vertical to horizontal dimensions of the cubic compression space of IRIS-15. The horizontal dimension increased with respect to the vertical one with increasing press load at a rate of 22 μm/MN. It was suppressed to −0.07 μm/MN by trial-and-error adjustments.

TABLE I. Comparison of properties of carbides used for anvil material of multi-anvil experiments.

Company	Hawedia	Fujilloy	
Type	ha-co6%	TF05	TF09
Vickers Hardness (MPa)	2040	2280	1760
Rockwell hardness A[a]	94.5	>94	93.0
Compressional strength (GPa)[a]	>7	6.7	6.1

[a]These values are taken from catalogues of the above companies.

material is WC cemented by cobalt. In general, the hardness of the carbide increases with decreasing cobalt content. Table I summarizes Vickers hardness, Rockwell hardness A scale, and compressional strength of several carbide materials (Hawedia ha-co6%, Fujilloy TF09 and Fujilloy TF05). It was found that Fujilloy TF05 has the highest Vickers hardness among them. Because it is well-known that the TF05 anvil has relatively small amounts cobalt-binder and it is not only harder but also more fragile, this kind of ultra-hard tungsten carbide anvil has the problem for repeated use. However, it has been used for experiments which needed higher pressures than before over years.[13,14] Pressures generated using the WC anvils with 3.0-mm truncation in combination with MgO + 5 wt. % Cr_2O_3 pressure media with an edge length of 7.0 mm are compared by detecting the electrical resistance changes associated with the I-II (2.55 GPa[1,15]) and III-V (7.7 GPa[1,15]) metal-metal transitions of Bi and semiconductor-metal transitions of ZnS (15.6 GPa[1,15]) and GaP (23 GPa[1,15]) (Fig. 4). The results clearly show the highest performance of pressure generation by Fujilloy TF05, especially above 20 GPa. Therefore, we have adopted this carbide material for the further experiments.

B. Tapering of anvil

A major reason for the limitation of pressure generation with any anvil materials is yielding of anvils, especially around the truncation. Even though the press load is increased, just the truncated corners of anvils yield and the high-pressure volume formed by the inner anvils is not decreased. In other words, stress concentration into the center of sample part needs to be kept to generate higher pressure so as not to be dispersed it by the deformation of anvil top. In order to overcome this problem, three anvil faces around the truncation are tapered by 1.0° in this study. This technique is essentially the same as the "bevel" of diamond anvil cells.[16] The three faces, opposite to the truncation, meet each other at right angles (Figs. 5(a) and 5(b)). The tapering of the anvil faces is not a new technique for KMAP, but was already adopted by Ref. 17 about 40 years ago. We compared generated pressures by using normal-type (no-tapered or flat) and 1.0°-tapered anvils of 1.5 mm truncations in combination with MgO + 5 wt. % Cr_2O_3 pressure media with edge length of 5.7 mm. The generated pressures at ambient temperature were first examined using IRIS-15 by detecting the electric resistance changes associated with the following phase transitions: ZnS semiconductor-metal (15.6 GPa[1,15]), GaP semiconductor-metal (23 GPa[1,15]) and Zr α-ω (8 GPa[18,19]), and Zr ω-β (34 GPa[18,19]). Fig. 5(c) shows comparison of pressure generation using anvils with 1.5 mm truncation with and without tapering at ambient temperature. As is seen, the ω-β transitions of Zr occur at 10.8 MN and 7.5 MN using flat and tapered anvils, respectively, demonstrating that the tapered anvils have higher efficiency in pressure generation than the flat anvils.

IV. PRESSURE GENERATIONS OVER 40 GPA

The anvils adopted throughout this section were Fujilloy TF05 with 1.5 mm truncation and 1.0° tapering. The pressure media were octahedral semi-sintered MgO + 5 wt. % Cr_2O_3 with edge length of 5.7 mm, and gaskets with 3.0-mm

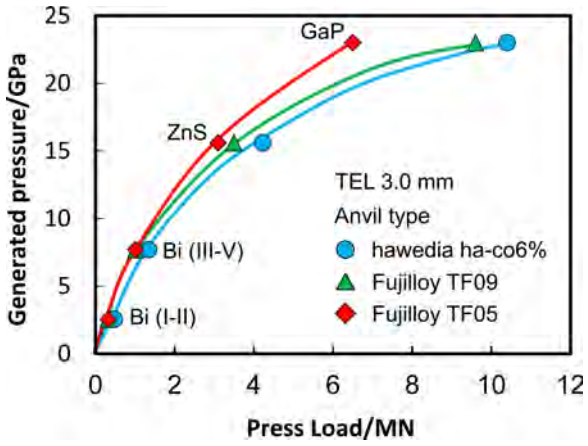

FIG. 4. Comparison of pressure generation at room temperature using carbide material hawedia ha-co6%, Fujilloy TF09, and Fujilloy TF05 with 3.0 mm truncation. Bi, ZnS, and GaP are pressure calibrants at room temperature. Solid circles, triangles, and diamonds are the results by hawedia ha-co6%, Fujilloy TF09, and Fujilloy TF05 anvils, respectively. TEL, truncated edge length.

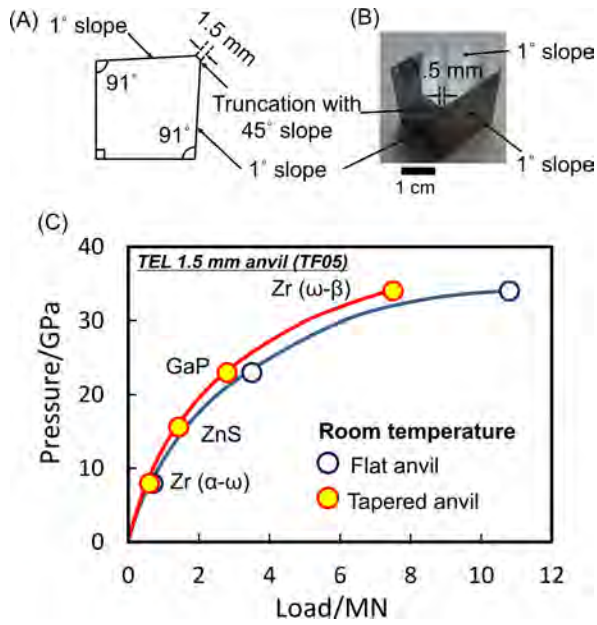

FIG. 5. Comparison of performances on pressure generation of flat and tapered anvils with 1.5 mm truncation (Fujilloy TF05) at room temperature. (a) and (b) Tapered anvils with 1.5 mm truncations as seen from [100] direction and [111] direction, respectively. (c) Pressure calibration curves at room temperature with flat and tapered anvils. ZnS, GaP, and Zr were pressure calibrants at room temperature. Solid circles and open circles are the results by flat and tapered anvils, respectively. TEL, truncated edge length.

width and 1.0-mm thickness were used in most runs. Runs at 2000 K using IRIS-15 adopted the pressure media with 6.8 mm edge length and gaskets with 3.0-mm width and 1.25-mm thickness. These gaskets have a slope at the top to accommodate the pressure medium without any special gap. High temperature was generated with a cylindrical joule heater placed in a pressure medium. Re and Mo foils were adopted as the heating elements. Temperatures were measured using a W3%Re-W25%Re thermocouple. In order to suppress applied electric power, $LaCrO_3$ was used as thermal insulator in runs at 2000 K with IRIS-15. Phases in samples recovered from high-pressure and high-temperature conditions were examined by using a micro-focused X-ray diffractometer (MFXRD), a field-emission scanning electron microscope (FE-SEM) with an energy-dispersive X-ray analyzer (EDX), and analytical transmission electron microscope (ATEM).

A. Pressure generation at ambient temperature

Generated pressures at ambient temperature were examined by *in situ* X-ray diffraction using SPEED-*Mk*.II. The schematic drawing of the high-pressure cell assembly is shown in Fig. 6(a). Energy dispersive X-ray diffraction by white X-ray beams collimated to 50 μm horizontally and 200 μm vertically was adopted at diffraction angle $2\theta = \sim 8°$ using a germanium solid-state detector (SSD). The diffracted X-ray was collected in an energy range up to ca. 160 keV calibrated using fluorescence of Cu, Mo, Ag, Ta, Pt, Au, and Pd. To minimize the effect of preferred orientation of samples, the press was oscillated between 0° and 8°.[9] The sample was a mixture of MgO and 5 wt. % of Au, and generated pressures were determined from relative volumes of Au and MgO, based on equation of states of Refs. 20 and 21, respectively. The sample was loaded in a Mo foil tube, which also worked as a heater. Al_2O_3 was placed in and out of the Mo foil tube. The reason for the loading of Al_2O_3 is that it has the much higher bulk modulus (~240 GPa[22]) than MgO (~160 GPa[22]).

Figure 7(a) shows results of examination of pressure generation by *in situ* X-ray diffraction experiment of SPEED-*Mk*.II together with those of IRIS-15. The generated pressures in this run were almost equivalent with those of IRIS-15 up to the press load of 6-7 MN. Above this press load, pressures generation was more efficient in the experiment conducted in SPEED-*Mk*.II, which may be due to the use of Al_2O_3 around the sample.[23] The generated pressure reached 43 GPa at the maximum press load of 15 MN.

B. Pressure generation at high temperatures

The lower-mantle mineral of bridgmanite (Brm), whose primary composition and structure are $MgSiO_3$ and orthorhombic perovskite, respectively. This phase coexists with Al_2O_3 corundum (Crn) at pressures higher than 26 GPa,[24] and the Al_2O_3 content in Brm coexisting with corundum increases with increasing pressure.[25] Therefore, the Al_2O_3 contents in Brm can be used as a pressure calibrant for high-temperature quench experiments above 26 GPa. The Al_2O_3 contents in Brm coexisting with Crn were calibrated as a function of pressure at 2000 K by Liu *et al.*,[27] who demonstrated that the Al_2O_3 content in Brm reached 25%, namely, pyrope composition ($Mg_3Al_2Si_3O_{12}$), at a pressure of 45 GPa.

We tried to synthesize Brm with the pyrope composition at a temperature of 2000 K and a press load of 15 MN (the maximum press load of the present apparatus). A schematic drawing of the cell assembly is shown in Fig. 6(b). The sintered akimotoite (ilmenite structure) with the pyrope composition (py-Ak) was used as a starting material to minimize drops in sample pressure due to volume reduction by the phase transition. The py-Ak was synthesized from glass with the pyrope composition (py-glass) using flat anvils with 3 mm truncation at 26 GPa and 1170 K.[25] The py-glass was synthesized from a mixture of MgO, Al_2O_3, and SiO_2 with 3:1:3 molar ratios, respectively, by melting at 1950 K for 1 h, and then quenching by falling it into water. Powdered py-glass was directly packed at the center of a Mo foil heater in a 5 wt. % Cr_2O_3-doped MgO octahedron with 7.0 mm edge length. The sintered py-Ak was loaded directly to a Re heater. The heater was then inserted into another cell assembly (Fig. 6(b)), where the majority of the pressure

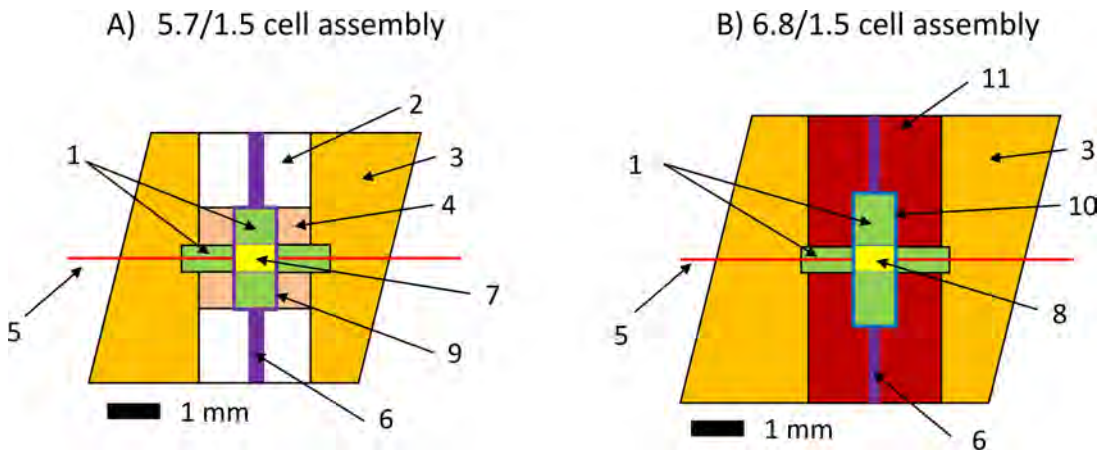

FIG. 6. Schematic drawings of high-pressure cell assemblies for the pressure generation tests. (a) For *in situ* X-ray diffraction experiment and (b) quench experiment. (1) Dense alumina, (2) MgO, (3) MgO + 5 wt. % Cr_2O_3 pressure medium, (4) crushable alumina sleeve, (5) W3%Re-W25%Re thermocouple, (6) Mo electrode, (7) sample (MgO + 5 wt. % Au), (8) sample (sintered ilmenite-type $Mg_3Al_2Si_3O_{12}$), (9) Mo heater, (10) Re heater, and (11) $LaCrO_3$ thermal insulator. 5.7/1.5 and 6.8/1.5 are octahedral edge length of pressure medium/truncated edge length of inner anvil.

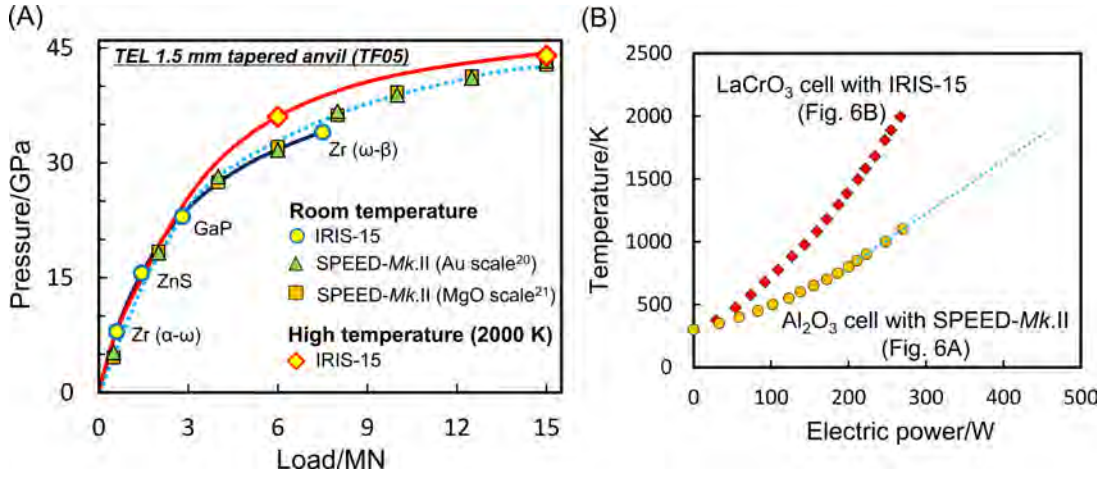

FIG. 7. (a) Pressure generation using TF05 anvils with 1.5 mm truncation and 1° tapered faces at room temperature and high temperature (2000 K). Circles and diamonds are pressure generated with IRIS-15 at room temperature and 2000 K, respectively. Triangles and squares are pressure generated with SPEED-*Mk*.II at room temperature using equation of states of Au[20] and MgO,[21] respectively. Dotted line was drawn using triangles and squares. ZnS, GaP, and Zr were pressure calibrants at room temperature. TEL, truncated edge length. (b) Comparison of heating efficiencies of Al_2O_3 (Fig. 6(a)) and $LaCrO_3$ (Fig. 6(b)) cells. Circles and diamonds are correlations between the supply power to the heater and temperature of sample part in Al_2O_3 (Fig. 6(a)) and $LaCrO_3$ (Fig. 6(b)) cells, respectively. Electric powers extrapolated with those between 850 and 1100 K (dotted line) were supplied above 1100 K because thermocouple broke above 1100 K.

medium was replaced by a $LaCrO_3$ thermal insulator. $LaCrO_3$ is an opaque material, which should prevent radiative heat transfer to allow high-temperature generation with small electric power. The pressure medium was then compressed in IRIS-15 and heated to a stable temperature of 2000 K. As shown in Fig. 7(b), a comparison of heating efficiency between two high-pressure cell assemblies (Figs. 6(a) and 6(b)) demonstrates that the $LaCrO_3$ cell assembly (Fig. 6(b)) has 1.5 times higher heating efficiency at 1100 K than Al_2O_3 cell assembly without $LaCrO_3$ (Fig. 6(a)).

The resultant run product was not Brm but had a $LiNbO_3$ (LN) structure with $Mg_{3.06(3)}Al_{1.94(6)}Si_{3.01(3)}O_{12}$ composition. An SEM observation showed that there are tiny (1-2 μm) Al_2O_3-rich parts, which should indicate coexistence of Crn. Reference 26 reported that Brm with Al contents exceeding 0.5 atoms on a 3-oxygen basis such as natural garnet composition $(Mg,Fe,Ca)_3Al_2Si_3O_{12}$ cannot be recovered to ambient conditions, but transforms to a LN structure during decompression. A similar experiment with almost same power for heating to a temperature of 2000 K at a press load of 6 MN indicated that a recovered sample was a mixture of Brm with Al cation number of 1.59(2) with Crn: this Al_2O_3 content in this Brm indicates that the generated pressure was 36 GPa at this press load. This also supports the hypothesis that LN phase at 15 MN was formed by back transformation of Brm during decompression. Therefore, the LN-structured material with the $Mg_{3.06(3)}Al_{1.96(5)}Si_{3.00(2)}O_{12}$ composition recovered from the press load of 15 MN should have been Brm at the high pressure and temperature and indicates generation of ~44 GPa pressure. Details of the $Mg_{3.06(3)}Al_{1.94(6)}Si_{3.01(3)}O_{12}$ compound with the LN structure will be described elsewhere (Ishii *et al.*[28]). Figure 7(a) shows the pressure calibration curve at 2000 K. Here, we emphasize that the heating efficiency is essential for high-pressure generation with multi-anvil apparatus at high temperatures, because we also examined pressures generation with the cell assembly to generate high temperatures using a Mo heater with an Al_2O_3 sleeve for *in situ* X-ray diffraction (Fig. 6(a)), and found that the generated pressure monotonically decreased with increasing temperature from 43 GPa to ~36 GPa at 1100 K. Pressures at high temperature are changed by the balance between pressure elevation by thermal expansion of materials in high-pressure cells and pressure reduction by the enhanced flow of gaskets by high-temperature softening. We infer that the high-pressure generation of 44 GPa at the high temperature of 2000 K was realized by the thermal pressure overcoming the softening of gasket materials by the high heating efficiency due to the $LaCrO_3$ thermal insulator.

V. CONCLUSION

In this article, we demonstrate the pressure generation over 40 GPa using a KMAP with the WC anvils by combining available high-pressure techniques. The use of hard carbide material, anvil tapering and highly incompressible pressure-transmitting material effectively enhances pressure generation. At the maximum press load of 15 MN, maximum sample pressures reached 43 and 44 GPa at ambient pressure and high temperature of 2000 K, respectively.

ACKNOWLEDGMENTS

We thank H. Fischer, S. Übelhack, R. Njul, H. Schulze, and U. Trenz at University of Bayreuth and C. Oka at Okayama University for their technical assistance. We are grateful to the Associated Editor and reviewers for constructive comments and valuable suggestions. The synchrotron radiation experiments were performed at the BL04B1 of SPring-8 with the approval of the Japan Synchrotron Radiation Research Institute (JASRI) (Proposal No. 2015A1359). This study is also supported by the research project approved by DFG (Proposal Nos. KA3434/3-1, KA3434/6-1, and KA3434/7-1) and by the Research Fellowship from the Scientific Research of the Japan Society for the Promotion of Science (JSPS) for Young Scientists to T.I.

[1]E. Ito, in *Treatise on Geophysics*, edited by G. Schubert, B. Romanowicz, and A. Dziewonski (Elsevier, San Diego, 2007), p. 197.
[2]H. Keppler and D. Frost, in *Mineral Behaviour at Extreme Conditions*, edited by R. Miletich (Eötvös University Press, Budapest, 2005), p. 1.
[3]T. Ishii, H. Kojitani, and M. Akaogi, Earth Planet. Sci. Lett. **309**, 185 (2011).
[4]Y. Fukao and M. Obayashi, J. Geophys. Res.: Solid Earth **118**, 5920, doi:10.1002/2013JB010466 (2013).
[5]T. Katsura, S. Yokoshi, K. Kawabe, A. Shatskiy, M. A. G. M. Manthilake, S. Zhai, H. Fukui, H. A. C. I. Hegoda, T. Yoshino, D. Yamazaki, T. Matsuzaki, A. Yoneda, E. Ito, M. Sugita, N. Tomioka, K. Hagiya, A. Nozawa, and K.-i. Funakoshi, Geophys. Res. Lett. **36**, L01305, doi:10.1029/2008gl035658 (2009).
[6]Y. Tange, Y. Kuwayama, T. Irifune, K. Funakoshi, and Y. Ohishi, J. Geophys. Res. **117**, B06201, doi:10.1029/2011JB008988 (2012).
[7]F. Wang, Y. Tange, T. Irifune, and K. Funakoshi, J. Geophys. Res. **117**, B06209, doi:10.1029/2011JB009100 (2012).
[8]D. Yamazaki, E. Ito, T. Yoshino, N. Tsujino, A. Yoneda, X. Guo, F. Xu, Y. Higo, and K. Funakoshi, Phys. Earth Planet. Inter. **228**, 262 (2014).
[9]T. Katsura, K. Funakoshi, A. Kubo, N. Nishiyama, Y. Tange, Y. Sueda, T. Kubo, and W. Utsumi, Phys. Earth Planet. Inter. **143**, 497 (2004).
[10]J. Osugi, K. Shimizu, K. Inoue, and K. Yasunami, Rev. Phys. Chem. Jpn. **34**, 1 (1964).
[11]O. Shimomura, W. Utsumi, T. Taniguchi, T. Kikegawa, and T. Nagashima, in *High-Pressure Research: Application to Earth and Planetary Science*, edited by Y. Syono and M. H. Manghnani (Terra Scientific Publishing Company, Tokyo, 1992), p. 3.
[12]T. Irifune, Rev. High Pressure Sci. Technol. **20**, 158 (2010).
[13]T. Kawazoe, N. Nishiyama, Y. Nishihara, and T. Irifune, High Pressure Res. **30**, 167–174 (2010).
[14]K. D. Litasov, E. Ohtani, A. Suzuki, and K. Funakoshi, Phys. Chem. Miner. **34**, 159–167 (2007).
[15]K. J. Dunn and F. P. Bundy, Rev. Sci. Instrum. **49**, 365–370 (1978).
[16]H. K. Mao and P. M. Bell, Carnegie Inst. Washington Yearb. **76**, 644 (1977).
[17]E. Ito, Geophys. Res. Lett. **4**, 72, doi:10.1029/GL004i002p00072 (1977).
[18]Y. Tange, E. Takahashi, and K. Funakoshi, High Pressure Res. **31**, 413 (2011).
[19]S. Ono and T. Kikegawa, J. Solid State Chem. **225**, 110 (2015).
[20]M. Yokoo, N. Kawai, K. G. Nakamura, K. Kondo, Y. Tange, and T. Tsuchiya, Phys. Rev. B **80**, 104114 (2009).
[21]Y. Tange, Y. Nishihara, and T. Tsuchiya, J. Geophys. Res. **114**, B03208, doi:10.1029/2008JB005813 (2009).
[22]N. Soga and O. L. Anderson, J. Am. Ceram. Soc. **49**, 355–359 (1966).
[23]Y. Tange, T. Irifune, and K. Fnakoshi, High Pressure Res. **28**, 245–254 (2008).
[24]T. Irifune, T. Koizumi, and J. I. Ando, Phys. Earth Planet. Inter. **96**, 147 (1996).
[25]A. Kubo and M. Akaogi, Phys. Earth Planet. Inter. **121**, 85 (2000).
[26]N. Funamori, T. Yagi, N. Miyajima, and K. Fujino, Science **275**, 513 (1997).
[27]Z.-D. Liu *et al.*, "Phase relations in the system $MgSiO_3$-Al_2O_3 to 52 GPa and 2000 K" (unpublished).
[28]T. Ishii *et al.*, "Crystal structure of $LiNbO_3$-type $Mg_3Al_2Si_3O_{12}$" (unpublished).